SUPPORTING INFORMATION

In situ growth of copper-based energetic complexes on GO and MXene to synergistically promote the thermal decomposition of ammonium perchlorate

Shuting Li,[a] Min Li,[a] Jinxi Han,[a] Zhengqiang Xia,[a] Sanping Chen,[a]* Gang Xie,[a] Shengli Gao,[a] Jack Y. Lu,[b] Qi Yang [a]*

[a]*Key Laboratory of Synthetic and Natural Functional Molecule of the Ministry of Education, College of Chemistry and Materials Science, Northwest University, Xi'an, Shaanxi, 710127, P. R. China.*

[b]*Department of Chemistry, University of Houston-Clear Lake, 2700 Bay Area Blvd. Houston,TX 77058, U.S.A.*

**Corresponding authors e-mail address: yangqi@nwu.edu.cn, sanpingchen@126.com*

Table of Contents

Section S1 Experimental Procedures

Experimental

Caution: The target energetic complexes are hazardous materials, which may occur explosion under specific conditions. The necessary safety precautions (safety glasses, face shield and plastic spatula) should be used during the experiment, especially when the products are prepared on a large scale.

Instruments

The data for the elemental analysis were collected using a Vario EL III analyzer. Thermogravimetric analysis (TGA) and differential scanning calorimetry (DSC) were carried out using a Netzsch STA 449C instrument and a CDR-4P thermal analyzer from Shanghai Balance Instrument factory, respectively, using dry oxygen-free nitrogen as the atmosphere, with a flow rate of 10 mL min^{-1}. About 0.8 mg of sample was sealed in an aluminum pan and a heating rate of 10 °C min^{-1} was used for TG and DSC measurements. The specific heat capacity (C_p) was measured using the continuous C_p mode of a C80 micro-calorimeter (Seteram Co., France). The sensitivity to impact stimuli is determined by the fall hammer apparatus applying the standard staircase method using a 2 kg drop weight, and the results are reported in terms of height for a 50% probability of explosion (H_{50}%). The friction sensitivity is determined on Julius Peter's apparatus by following the BAM method. The purity of the bulk samples was verified by X-ray powder diffraction (XRD) measurements on a RU 200 diffractometer (Rigaku Co., Japan) at 60 kV, 300 mA, and Cu *K*α radiation (λ = 1.5406 Å). Scanning electron microscope (SEM) image was performed/operated/recorded on an FEI Quanta 400 FEG at an acceleration voltage of 5 kV. X-ray photoelectron spectroscopy (XPS) was recorded on a Thermo Scientific Escalab Xi+ instrument.

Crystallographic data collection and refinement

The single-crystal X-ray diffraction data of EC-Cu1 and EC-Cu2 were collected by using a Bruker Smart Apex CCD diffractometer equipped with graphite monochromatized Cu *K*α radiation (λ = 0.71073 Å) using ω and φ scan modes. The

single crystal structures were solved by direct methods using SHELXS and refined by means of full-matrix least-squares procedures on F^2 with SHELXL program[1]. All non-H atoms were located using subsequent Fourier-difference methods and refined anisotropically. Other details of crystal data, data collection parameters and refinement statistics of EC-Cu1 and EC-Cu2 were given in Table S1. Selected bond lengths and bond angles of EC-Cu1 and EC-Cu2 were listed in Table S2 and Table S3, respectively. Hydrogen bond lengths and angles of EC-Cu1 and EC-Cu2 were listed in Table S4.

Table S1. Crystal data and structure refinement details of EC-Cu1 and EC-Cu2*

Crystal	EC-Cu1	EC-Cu2
Empirical formula	$C_6H_8CuN_{18}O_2$	$C_{12}H_{10}Cu_3N_{36}O_2$
CCDC number	1845998	1848504
Formula weight	427.84	881.18
Crystal system	Triclinic	Triclinic
Space group	*P*-1	*P*-1
Measurement temperature	296	150
a/ Å	6.8830(18)	6.3422(11)
b/ Å	9.131(3)	7.9744(13)
c/ Å	12.186(3)	13.452(2)
α/°	101.122(4)	73.360(8)
β/°	103.119(5)	84.082(9)
γ/°	106.744(4)	75.297(8)
V/Å^3	686.3(3)	630.15(18)
Z	2	1
$\rho_{calc.}$/g cm^{-3}	2.070	2.322
μ/mm^{-1}	1.653	2.611
F(000)	430.0	437.0
GOOF on F^2	1.027	1.012
R_1/wR_2 [$I>2\sigma(I)$]	0.0459/0.967	0.0532/0.1217
R_1/wR_2 [all data]	0.0703/0.1057	0.0983/0.1447

* $R_1 = \Sigma\left||F_0|-|F_c|\right| / \Sigma|F_0|, wR_2 = [\Sigma(F_0^2 - F_c^2) / \Sigma w(F_0)^2]^{1/2}$

Table S2. Selected bond lengths of EC-Cu1 and EC-Cu2.

	Atom	Atom	Length/Å	Atom	Atom	Length/Å
EC-Cu1	Cu1	N2	2.098(3)	Cu1	N4	1.894(4)
	Cu1	N18	1.901(3)	Cu1	O1	2.004(4)
	Cu1	O2	2.367(4)			
EC-Cu2	Cu1	N4	1.935(5)	Cu1	N3	2.297(5)
	Cu1	N14#3	2.109(5)	Cu1	N9	1.937(5)
	Cu1	N17#4	2.205(5)	Cu2	O1#1	2.364(4)
	Cu2	N5#1	1.990(5)	Cu2	N15#2	2.004(5)

#1 1-X,1-Y,2-Z; #2 +X,+Y,1+Z; #3 1-X,1-Y,1-Z; #4 -X,1-Y,1-Z

Table S3. Selected bond angles of EC-Cu1 and EC-Cu2.

	Atom	Atom	Angle/°	Atom	Atom	Atom	Angle/°
EC-Cu1	N4	N18	173.77(16)	N4	Cu1	O1	89.21(15)
	N18	O1	87.70(15)	N4	Cu1	N2	91.25(14)
	N18	N2	90.80(15)	O1	Cu1	N2	169.40(15)
	N4	O2	93.23(14)	N18	Cu1	O2	92.53(14)
	O1	O2	97.46(14)	N2	Cu1	O2	93.08(13)
	C3	Cu1	123.6(3)	C2	N2	Cu1	123.3(3)
	C4	Cu1	128.8(3)	N5	N4	Cu1	125.6(3)
	C5	Cu1	127.9(3)				
EC-Cu2	N4	N14	87.3(2)	N4	Cu1	N9	173.2(2)
	N3	N4#2	87.03(19)	N4	Cu1	N17#4	84.7(2)
	N14#2	N3	121.83(19)	N14#2	Cu1	N17#4	147.3(2)
	N9	N14#2	93.4(2)	N9	Cu1	N3	86.91(19)
	N9	N17#4	98.2(2)	N17#4	Cu1	N3#2	89.38(19)
	N5	Cu1	125.9(4)	C4	N4	Cu1	129.1(4)
	N15	Cu1#2	123.7(4)	C6	N14	Cu1#2	132.0(4)
	N15#2	O1#1	92.69(18)	N15#2	Cu2	O1	87.31(18)
	N5	O1	93.29(18)	N5#1	Cu2	O1#1	86.71(18)
	N5#1	N15#3	89.7(2)	N5#1	Cu2	N15#2	90.3(2)
	N14	Cu2#5	126.6(4)	N16	N15	Cu2#5	123.4(4)
	N4	Cu2	126.5(4)	N6	N5	Cu2	122.2(4)

Table S4. Hydrogen bond lengths (Å) and angles (°) of EC-Cu1 and EC-Cu2.

	D-H···A	d(D-H)/Å	d(H-A)/Å	d(D-A)/Å	D-H-A/°
EC-Cu1	N9-H9···N3	0.86(3)	2.34(2)	2.826(5)	116(5)
	N9-H9···N7#1	0.86(3)	2.04(6)	2.747(6)	138(5)
	N13-H13···N12#2	0.86(3)	2.00(8)	2.862(6)	172(3)
	N14-H14···N6#1	0.86(3)	1.93(6)	2.793(6)	174(4)
	O1-H1A···O2#3	0.84(4)	1.88(5)	2.716(5)	168(5)
	O1-H1B···N17#3	0.84(3)	2.16(6)	2.771(6)	130(5)
	O2-H2A···N16#4	0.85(3)	1.99(7)	2.832(6)	168(7)
	O2-H2B···N15#4	0.84(5)	2.08(5)	2.897(5)	165(5)
	O2-H2A···N17#5	0.85(3)	2.69(3)	3.393(5)	140(3)
	O2-H2B···N16#4	0.84(3)	2.68(2)	3.364(5)	139(4)
#1 X-1,Y-1, Z; #2 -X+2,-Y-1,-Z; #3 -X+2,-Y+1,-Z+1; #4 -X+1,-Y,-Z+1; #5 X+1,Y, Z					
EC-Cu2	O1-H1A···N14#1	0.87(3)	2.66(2)	3.171(5)	118(5)
	O1-H1A···N17#2	0.87(3)	2.66(2)	3.130(5)	114(4)
	O1-H1B···N16#2	0.87(3)	2.27(2)	2.963(6)	135(4)
	N18-H2···N7#3	0.88(3)	1.92(3)	2.749(8)	156(5)
	N13-H3···N12#4	0.88(3)	2.36(2)	3.238(6)	171(5)
	N8-H1···N1#3	0.88(3)	2.46(2)	3.311(8)	162(4)
#1 1-X,1-Y,1-Z; #2 -X,1-Y,1-Z; #3 -X,2-Y,1-Z; #4 1-X,-Y,1-Z					

Section S2 Results and discussion

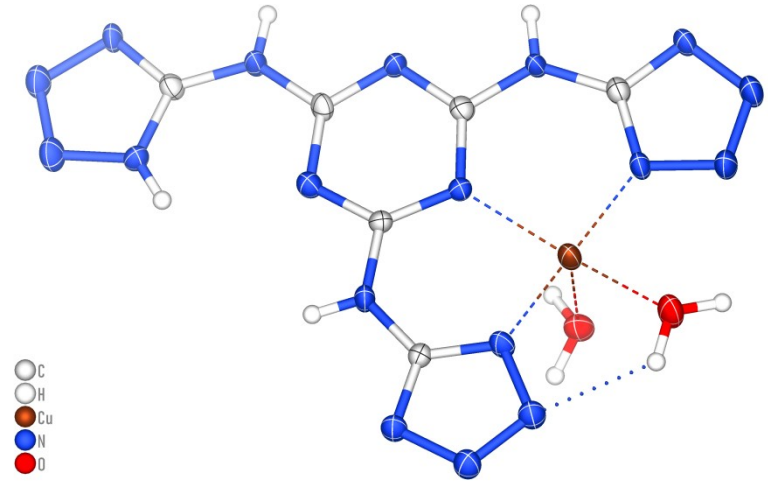

Figure S1. Molecular structure of EC-Cu1. Anisotropic displacement parameters are depicted at the 50% probability level.

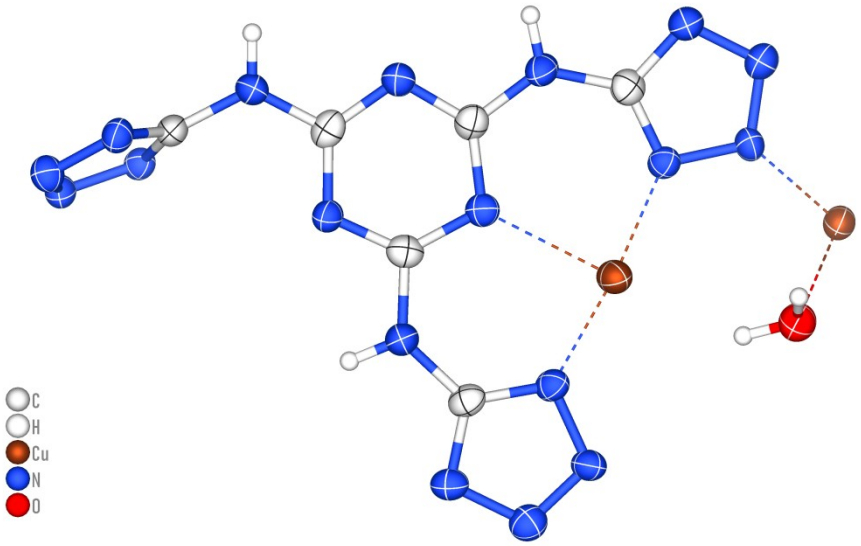

Figure S2. Molecular structure of EC-Cu2. Anisotropic displacement parameters are depicted at the 50% probability level.

Heat of detonation

Density functional theory (DFT) was used to preliminary estimate the energy of detonation (ΔE_{det}), from which the heat of detonation (ΔH_{det}) is calculated by using a linear correlation equations ($\Delta H_{det} = 1.127\Delta E_{det} + 0.046$, $r = 0.968$), which is widely used to estimate the heat of detonation of explosives [2,3]. For EC-Cu1 and EC-Cu2, water, ammonia, nitrogen and carbon were assumed to be the final products of decomposition of organic components. The formation of metal oxide was assumed to be governed by the content of oxygen, meanwhile, metal atom can be treated as its reduction state, if the heat of formation of metallic oxide is higher than that of water. In addition to zinc oxide, lead and carbon, the rest of final products are considered as gas phase. The complete detonation reactions of EC-Cu1 and EC-Cu2 are described by equation (1) and (2) and the calculated parameters used in the detonation reactions as shown in Table S5.

$$CuC_6H_8N_{18}O_2 \rightarrow Cu + 2H_2O + \frac{4}{3}NH_3 + 6C + \frac{25}{3}N_2 \quad (1)$$

$$Cu_3C_{12}H_{10}O_2N_{36} \rightarrow 3Cu + 2H_2O + 2NH_3 + 12C + 17N_2 \quad (2)$$

It is known that the energy of materials comes from energy units. For EC-Cu1 and EC-Cu2, a minimum asymmetric unit contains one energy ligand molecules, but EC-Cu2 contains one and a half copper ions, which makes its effective energy component relatively small. Therefore, the heat of detonation of EC-Cu1 ($\Delta H_{det} = 4.279$ kcal g^{-1}) is higher than that of EC-Cu2 ($\Delta H_{det} = 4.067$ kcal g^{-1}).

Table S5. The calculated parameters used in the detonation reactions

	ECs (hartree)	Cu (hartree)	H_2O (hartree)	NH_3 (hartree)	C (hartree)	N_2 (hartree)	ΔE_{det} (hartree)	ΔE_{det} (kcalg^{-1})	ΔH_{det} (kcalg^{-1})
1	-1565.265	-196.113	-76.378	-56.505	-37.738	-109.448	2.561	3.756	4.279
2	-3172.587	-196.113	-76.378	-56.505	-37.738	-109.448	5.010	3.568	4.067

Detonation performance

The detonation characteristics of energetic materials can be evaluated by its detonation velocity (D) and detonation pressure (P). Herein, the empirical Kamlet–Jacobs equations (3)-(5) were employed to estimate the values of D and P[4], which have been proved by numerous studies as the most reliable approach among the empirical methods[5].

$$D = 1.01\Phi^{1/2}(1+1.30\rho) \quad (3)$$

$$P = 1.558\Phi\rho^2 \quad (4)$$

$$\Phi = 31.68N(MQ)^{1/2} \quad (5)$$

Where D is detonation velocity (km s^{-1}), P is detonation pressure (GPa), ρ is the density of explosive (g cm^{-3}), N is the moles of detonation gases per gram of explosive, M is the average molecular weight of these gases and Q is the heat of detonation (kcal g^{-1}). The calculated parameters and results of D and P are listed in Table S6.

Table S6. Calculated parameters of detonation velocity and detonation pressure of EC-Cu1 and EC-Cu2.

	ρ (g cm^{-3})	N (mol g^{-1})	M (g mol^{-1})	Q (kcal g^{-1})	D (km s^{-1})	P (GPa)
EC-Cu1	2.070	0.027	25.028	4.279	11.10	59.10
EC-Cu2	2.322	0.024	26.000	4.067	11.35	65.68

The theoretical calculation results indicate that both EC-Cu1 and EC-Cu2 have good detonation performance. It should be noted that there may be some discrepancies between the predicted value and the experimental value, and it is only used as a basis for comparison between EC-Cu1 and EC-Cu2.

Sensitivity tests

For safety reasons during the uses and further testing of EC-Cu1 and EC-Cu2, their impact and friction sensitivities were respectively carried out. The impact sensitivity was measured by a fall hammer apparatus. A 2.0 kg weight was dropped from a set height onto a 20 mg sample at a 39.2 MPa press. The test results show that title complexes don't fire at the highest point of 200 cm, which corresponds to the impact energy of 40 J. Meanwhile, no friction sensitivities of EC-Cu1 and EC-Cu2 were observed up to 36 kg (360 N). The above results indicate that EC-Cu1 and EC-Cu2 are insensitive to impact and friction stimuli. The physicochemical properties of EC-Cu1, EC-Cu2, and some classical energetic materials are listed in Table S7.

Table S7. The physicochemical properties of EC-Cu1, EC-Cu2 and some classical energetic materials.

	ρ^a (g cm^{-3})	N^b (%)	Ω^c (%)	$T_d{}^d$ (^{o}C)	Q^e (kcal g^{-1})	D^f (km s^{-1})	P^g (GPa)	IS^h (J)	FS^i (N)
EC-Cu1	2.070	58.90	-52.36	335	4.279	11.10	59.10	>40	>360
EC-Cu2	2.322	57.19	-49.02	352	4.067	11.35	65.68	>40	>360
$[Cu(Htztr)_2(H_2O)_2]_n$[5]	1.892	52.72	-60.24	345	2.1281	8.18	30.57	>40	>360
$\{[Cu(tztr)]\cdot H_2O\}_n$[5]	2.316	45.23	-48.00	325	1.3220	7.92	31.99	>40	>360
$[Cu(Htztr)]_n$[5]	2.435	49.08	-56.09	355	3.9582	10.40	56.48	32	>360
$\{[Cu(Htztr)(H_2O)]NO_3\}_n$[6]	2.242	40.04	-5.72	302	2.1272	9.22	42.56	>40	>360
$[Cu(H_2tztr)_2(HCOO)_2]_n$[6]	1.884	45.81	-29.78	338	3.5663	9.28	39.21	>40	>360
TNT[7]	1.65	18.50	-24.67	295	1.158	7.303	21.30	15.0	353
RDX[7]	1.80	37.84	-21.61	205	0.897	8.795	34.90	7.5	120
HMX[5]	1.91	37.84	-21.61	275	1.386	8.900	38.39	7.0	112

[a] Density from X-ray diffraction analysis, [b] Nitrogen content, [c] Oxygen balance, [d] Temperature of decomposition by DSC, [e] Heat of detonation, [f] Detonation velocity, [g] Detonation pressure, [h] Impact sensitivity, [i] Friction sensitivity.

X-ray photoelectron spectroscopy (XPS)

The survey spectrum (Figure S3a) shows the presence of C, N, O, and Cu in GCu1. In the C 1s region, the peaks at 288.4 eV, 285.8 eV, 285.2 eV, and 284.7 eV were attributed to C-O-Cu, C−O/O-C-O, C-N, and C-C, respectively (Figure S3b). The N 1s spectrum (Figure S3c) was fitted into three characteristic nitrogen species located at 400.8 eV, 400.6 eV, and 399.8 eV, ascribing to N^+, N-H/-N-N- and=N-, respectively. For the O 1s XPS profile, the peaks at 533.4, 532.1 and 530.6 eV could be assigned to -COOR, O-C=O/-COOH/-OH, and C=O respectively (Figure S3d). Similarly, it indicates that there are two peaks on the Cu $2p_{3/2}$ curves at 932.4 eV and 935.3 eV, which are labeled as Cu-N and C-O-Cu bonds, respectively. (Figure S3e)[2,3]

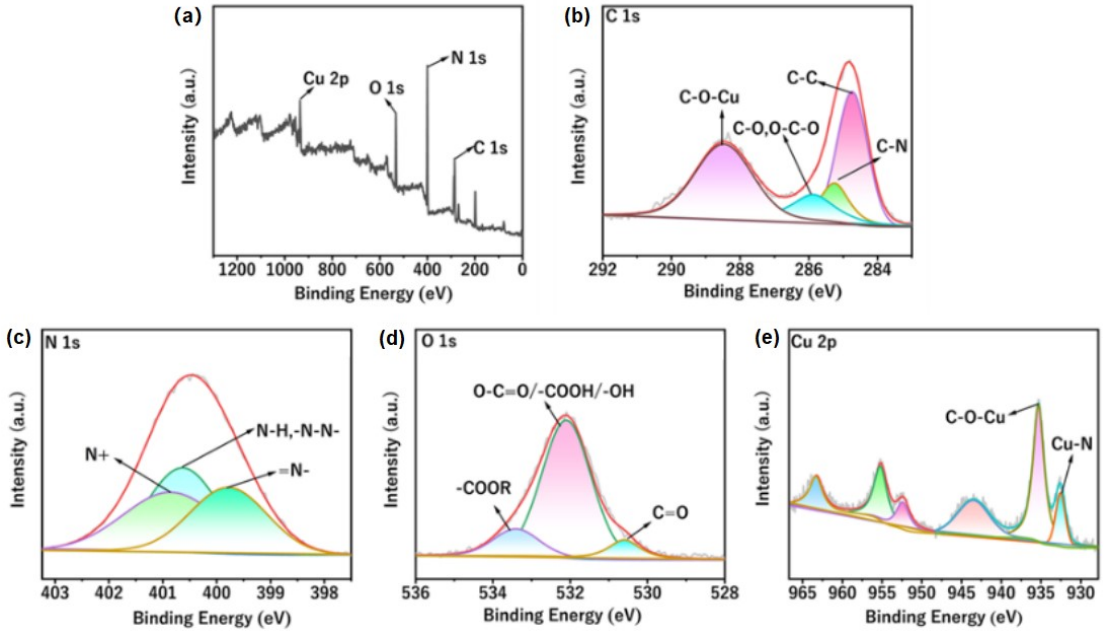

Figure S3. (a) XPS total spectrum of GCu1; (b-e) Highresolution XPS spectrum of C 1s, N 1s, O 1s, and Cu 2p of GCu1.

The survey spectrum (Figure S4a) shows the presence of C, N, O, Ti, and Cu in MCu1. In the C 1s region, the 284.8 eV, 286.6 eV and 288.4 eV peaks were attributed to C-C, C-O, and O=C-O, respectively (Figure S4b). The N 1s spectrum (Figure S4c) was fitted into three characteristic nitrogen species located at 400.9 eV, 400.5 eV, and 399.1 eV, ascribing to graphitic N, pyrrolic N, and pyridinic N, respectively. For the O 1s XPS profile, the peaks at 533.3 eV, 532.4 eV, 531.5 eV, and 530.4 eV could be assigned to Ti-O of TiO_2, C-Ti-O_x, C-Ti-$(OH)_x$, and H_2O, respectively (Figure S4d). The Ti 2p XPS profile (Figure S4e) has only two peaks at approximately 459.3 eV (Ti $2p_{3/2}$) and 465 eV (Ti $2p_{1/2}$) corresponding to Ti-O bonds in TiO_2. In the Cu 2p region, the peaks at 932.79 eV and 935.3 eV were assigned to Cu-N and C-O-Cu bonds, respectively. (Figure S4f)[4].

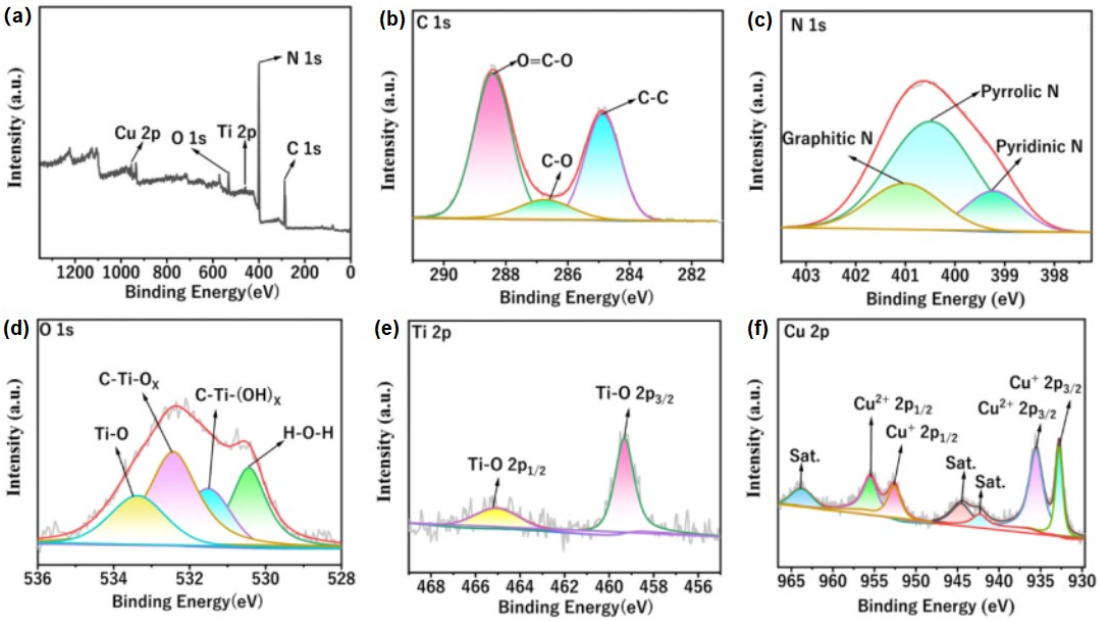

Figure S4. (a) XPS total spectrum of MCu1; (b-f) Highresolution XPS spectrum of C 1s, N 1s, O 1s, Ti 2p, and Cu 2p of MCu1.

Table S8. The results of promoting AP thermal decomposition by different samples.

Samples	T_{LTD} / ℃	T_{HTD} / ℃	ΔH (J g^{-1})
AP	343.7	445.3	465
EC-Cu1/AP	322.5	379.8	936
EC-Cu2/AP	316.4	382.9	2580
GCu1/AP-4	336.3	353.0	1068
GCu1/AP-6	341.2	-	1596
GCu1/AP-8	322.1	384.7	2514
GCu1/AP-10	335.6	354.7	1462
GCu2/AP-4	316.1	-	1324
GCu2/AP-6	322.6	-	1533
GCu2/AP-8	308.9	327.6	4875
GCu2/AP-10	320.4	-	1228
MCu1/AP-4	341.2	375.1	1502
MCu1/AP-6	337.1	370.0	1096
MCu1/AP-8	289.9	333.8	2185
MCu1/AP-10	346.2	-	1071
MCu2/AP-4	318.7	-	1048
MCu2/AP-6	323.6	-	2741
MCu2/AP-8	308.6	324.0	2265
MCu2/AP-10	313.7	-	1048

References

[1] G. M. Sheldrick, SHELXL, University of Göttingen, Germany, 2014.

[2] O.S. Bushuyev, B. Preston, M. Amitesh, R.H. Gee, G.R. Peterson, B.L. Weeks, L.J. Hope-Weeks, *J. Am. Chem. Soc.*, 2012, **134**, 1422-1425.

[3] J. Qin, J. Zhang, M. Zhang, D. Du, J. Li, Z. Su, Y. Wang, S.P. Pang, S.H. Li, Y. Lan, *Adv. Sci.*, 2015, **2**, 1500150.

[4] M.J. Kamlet, S.J. Jacobs, *J. Chem. Phys*., 1968, **48**, 23-35.

[5] X.Y. Liu, W.J. Gao, P.P. Sun, Z. Su, S.P. Chen, Q. Wei, G. Xie, S.L. Gao, *Green Chem.*, 2015, **17**, 831-836.

[6] X. Li, Q. Yang, Q. Wei, G. Xie, S.P. Chen, S.L. Gao, *Dalton Trans.*, 2017, **46**, 12893-12900.

[7] R. Meyer, J. Köhler, A. Homburg, Explosives, Wiley-VCH, Weinheim, 6th edn., 2007.